Direct spectral phase retrieval of ultrashort pulses by double modified one-dimensional autocorrelation traces

Shang-Da Yang*[1], Chen-Shao Hsu[1], Shih-Lun Lin[1], Houxun Miao[2], Chen-Bin Huang[1,2], Andrew. M. Weiner[2]

[1]*Institute of Photonics Technologies, National Tsing Hua University, Hsinchu 30013, Taiwan*

[2]*School of Electrical and Computer Engineering, Purdue University, West Lafayette, Indiana 47907-1285*

**Corresponding author: shangda@ee.nthu.edu.tw*

Abstract: We propose and experimentally demonstrate an original method to analytically retrieve complete spectral phase of ultrashort pulses by measuring two modified interferometric field autocorrelation traces using thick nonlinear crystals with slightly different central phase-matching wavelengths. This new scheme requires no spectrometer, detector array, nor iterative data inversion, and is compatible with periodically poled lithium niobate (PPLN) waveguide technology offering potential for high measurement sensitivity.

OCIS codes: (320.7100) Ultrafast measurements; (190.7110) Ultrafast nonlinear optics; (120.3180) Interferometry.

References and links

1. N. Dudovich, D. Oron, and Y. Silberberg, "Single-pulse coherently controlled nonlinear Ramman spectroscopy and microscopy," Nature (London) **418,** 512–514 (2002).
2. M. Yamashita, K. Yamane, and R. Morita, "Quasi-automatic phase-control technique for chirp compensation of pulse with over-one-octave bandwidth–generation of few to mono-cycle optical pulses," IEEE J. Quantum Electron. **16,** 213–222 (2006).
3. J. W. Nicholson, J. Jasapara, W. Rudolph, F. G. Omenetto, and A. J. Taylor, "Full-field characterization of femtosecond pulses by spectrum and cross-correlation measurements," Opt. Lett. **24,** 1774–1776 (1999).
4. R. Trebino, in *Frequency-Resolved Optical Gating: The Measurement of Ultrashort Laser Pulse*, (Kluwer Academic Publisher, Boston, MA, 2000).
5. I. Amat-Roldan, I. G. Cormack, P. Loza-Alvarez, and D. Artigas, "Measurement of electric field by interferometric spectral trace observation," Opt. Lett. **30,** 1063–1065 (2005).
6. C. Iaconis and I. A. Walmsley, "Spectral phase interferometry for direct electric-field reconstruction of ultrashort optical pulses," Opt. Lett. **23,** 792–794 (1998).
7. A. M. Weiner, "Effect of group velocity mismatch on the measurement of ultrashort optical pulses via second harmonic generation," IEEE J. Quantum Electron. **19,** 1276–1283 (1983).
8. P. O'Shea, M. Kimmel, X. Gu, and R. Trebino, "Highly simplified device for ultrashort-pulse measurement," Opt. Lett. **26,** 932–934 (2001).
9. S. -D. Yang, A. M. Weiner, K. R. Parameswaran, and M. M. Fejer,"400-photon-per-pulse ultrashort pulse autocorrelation measurement with aperiodically poled lithium niobate waveguides at 1.55 μm," Opt. Lett. **29,** 2070–2072 (2004).
10. S. -D. Yang, A. M. Weiner, K. R. Parameswaran, and M. M. Fejer, "Ultra-sensitive second-harmonic generation frequency-resolved optical gating by aperiodically poled $LiNbO_3$ waveguides at 1.5 μm," Opt. Lett. **30,** 2164–2166 (2005).

#103009 - $15.00 USD Received 21 Oct 2008; revised 20 Nov 2008; accepted 22 Nov 2008; published 26 Nov 2008

11. H. Miao, S. -D. Yang, C. Langrock, R. V. Roussev, M. M. Fejer, and A. M. Weiner,"Ultralow-power second-harmonic generation frequency-resolved optical gating using aperiodically poled lithium niobate waveguides," J. Opt. Soc. Am. B **25,** A41–A53 (2008).
12. S. -D. Yang, H. Miao, Z. Jiang, A. M. Weiner, K. R. Parameswaran, and M. M. Fejer, "Ultrasensitive nonlinear measurements of femtosecond pulses in the telecommunications band by aperiodically poled $LiNbO_3$ waveguides," Appl. Opt. **46,** 6759–6769 (2007).
13. A. S. Radunsky, E. M. Kosik Williams, I. A. Walmsley, P. Wasylczyk, W. Wasilewski, A. B. U'Ren, and M. E. Anderson, "Simplified spectral phase interferometry for direct electric-field reconstruction by using a thick nonlinear crystal," Opt. Lett. **31,** 1008–1010 (2006).
14. S. -D. Yang, S. -L. Lin and Y. -Y. Huang, "Complete spectral phase retrieval by modified interferometric field autocorrelation traces,"in Proc. Conf. Lasers and Elec. Optics (2008).
15. A. M. Weiner, Z. Jiang, and D. E. Leaird, "Spectrally phase-coded O-CDMA," J. Opt. Netw. **6,** 728–755 (2007).
16. I. Amat-Roldan, D. Artigas, I. G. Cormack, and P. Loza-Alvarez, "Simultaneous analytical characterization of two ultrashort laser pulses using spectrally resolved interferometric correlations," Opt. Express **14,** 4538–4551 (2006).
17. D. N. Fittinghoff, K. W. DeLong, R. Trebino, and C. L. Ladera,"Noise sensitivity in frequency-resolved optical-gating measurements of ultrashort pulses," J. Opt. Soc. Am. B **12,** 1955–1967 (1995).
18. K. W. DeLong and R. Trebino,"Improved ultrashort pulse-retrieval algorithm for frequency-resolved optical-gating," J. Opt. Soc. Am. A **11,** 2429–2437 (1994).
19. A. M. Weiner, *Ultrafast Optics* , (Wiley, in preparation).
20. K. R. Parameswaran, R. K. Route, J. R. Kurz, R. V. Roussev, and M. M. Fejer, "Highly efficient second-harmonic generation in buried waveguides formed by annealed and reverse proton exchange in periodically poled lithium niobate," Opt. Lett. **27,** 179–181 (2002).
21. J. Bethge and G. Steinmeyer,"Numerical fringe pattern demodulation strategies in interferometry," Rev. Sci. Instrum. **79,** 073102 (2008).

1. Introduction

Determination of spectral phase of ultrashort optical pulse is essential in a variety of applications, such as coherently controlled nonlinear spectroscopy [1], and adaptive pulse compression [2]. Ultrashort pulse characterizations normally rely on nonlinear optical effects to achieve ultrafast signal gating or spectral shearing. For example, phase and intensity from cross correlation and spectrum only (PICASO) [3], frequency-resolved optical gating (FROG) [4], measurement of electric field by interferometric spectral phase observation (MEFISTO) [5], and spectral phase interferometry for direct electric-field reconstruction (SPIDER) [6] have been demonstrated to measure spectral phase [5, 6] or complex field [3, 4]. These existing techniques, as commonly practiced, utilize a second harmonic generation nonlinearity, for which a sufficiently broad phase-matching (PM) spectrum (typically broader than the input pulse bandwidth) is needed in order to avoid measurement distortion. As a result, thin nonlinear crystals are routinely used in ultrashort pulse measurements [7], which however compromise the measurement sensitivity. Pulse measurement schemes using thick crystals have been reported. For example, FROG has been realized both by tight focusing of the input beam in a thick nonlinear crystal, which permits different frequency components of the short pulse to be phase matched at different angles [8], and by using a long crystal with a chirped quasi-phase matched grating, which permits different frequency components to be phase matched at different grating position [9, 10, 11, 12]. Nevertheless, the effective PM spectrum in these two schemes still has to be broader than the signal bandwidth (as in other methods). Long-crystal SPIDER uses the asymmetric group-velocity-mismatch condition in type II upconversion to produce spectrally sheared replicas, eliminating the need for a chirped auxiliary pulse [13]. This method simplifies the system configuration, but relies on particular combination of the crystal's material, length, and the wavelength range.

We have shown previously that using a thick nonlinear crystal with extremely narrow (δ -like) PM spectrum in a typical intensity autocorrelator will give rise to modified interferometric field autocorrelation (MIFA) trace [12]. Here we demonstrate an original scheme to directly (non-iteratively) reconstruct the spectral phase function by analyzing two MIFA traces meas-

#103009 - $15.00 USD Received 21 Oct 2008; revised 20 Nov 2008; accepted 22 Nov 2008; published 26 Nov 2008

ured at slightly different central PM wavelengths [14]. Our experimental setup can simultaneously retrieve the power spectrum without using a spectrometer. Furthermore, unlike previous techniques, this method can characterize a broadband signal using a genuinely narrowband PM mechanism. In terms of practical applications, MIFA scheme is reference-free, iteration-free and cost effective (requires no spectrometer and no detector array). Besides, like previous experiments using aperiodically-poled lithium niobate (A-PPLN) nonlinear waveguides which demonstrated record high sensitivity for pulse characterization at nanowatt average powers [9,10,11,12], MIFA is compatible with long nonlinear waveguide technology and therefore offers potential for very high measurement sensitivity. However, unlike previous techniques that required custom chirped A-PPLN nonlinear crystals, MIFA can be performed using (unchirped) periodically poled lithium niobate (PPLN) waveguide technology, which is commercially available.

2. Theory

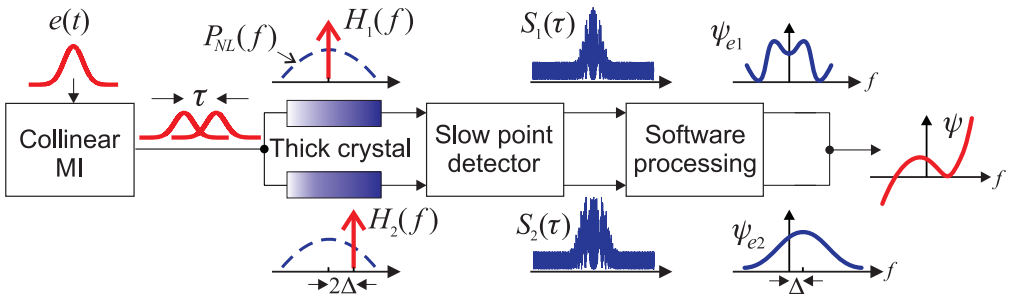

Fig. 1. Schematic diagram of MIFA measurement. MI: Michelson interferometer.

Figure 1 illustrates the schematic diagram of MIFA measurement. The scalar e-field of the pulse is represented by: $e(t) = \mathrm{Re}[a(t)\cdot\exp(j2\pi f_0 t)]$, where Re[ ] denotes real part, $a(t)$ is the complex temporal envelope, and f_0 represents carrier frequency, respectively. A collinear Michelson interferometer produces a pulse pair $e_\omega(t) = e(t) + e(t-\tau)$ (τ is variable delay), corresponding to a nonlinear polarization spectrum $P_{NL}(f) = F\{e_\omega^2(t)\}$ centered at $2f_0$ ($F\{\ \}$ denotes Fourier transform). By using a thick nonlinear crystal with narrow PM spectrum $H_1(f)$ centered at $2f_0$, the generated τ-dependent second-harmonic spectrum and average power are proportional to $P_{NL}(f)\cdot H_1(f) \propto P_{NL}(2f_0)$ and:

$$S_1(\tau) \propto 1 + 2|G_1'(\tau)|^2 + 4\mathrm{Re}[G_1'(\tau)]\cos(2\pi f_0\tau) + \cos(4\pi f_0\tau), \tag{1}$$

respectively, where the modified field autocorrelation function is defined as [12]:

$$G_1'(\tau) \equiv \langle a(t)a(t-\tau)\rangle / \langle a^2(t)\rangle. \tag{2}$$

The Fourier transform of Eq. (1), denoted by $\widetilde{S}_1(\kappa)$, consists of five spectral components centered at delay-frequencies of $\kappa = 0$, $\pm f_0$ and $\pm 2f_0$, respectively. By extracting the components centered at $\kappa = 0$ and $\kappa = f_0$, we can get the modulus and real part of $G_1'(\tau)$ ($|G_1'(\tau)|$ and $\mathrm{Re}[G_1'(\tau)]$), respectively. This enables determination of the complex function $G_1'(\tau)$ for the phase of $G_1'(\tau)$ can be evaluated by: $\angle|G_1'(\tau)| = \cos^{-1}\{\mathrm{Re}[G_1'(\tau)]/|G_1'(\tau)|\}$. The Fourier transform of Eq. (2) becomes:

$$\widetilde{G}_1'(f) \propto A(f)\cdot A(-f) = |A(f)\cdot A(-f)|\cdot\exp\{j[\psi(f)+\psi(-f)]\}, \tag{3}$$

#103009 - $15.00 USD Received 21 Oct 2008; revised 20 Nov 2008; accepted 22 Nov 2008; published 26 Nov 2008

where $A(f)=F\{a(t)\}=|A(f)|\times\exp[j\psi(f)]$ stands for the spectral envelope of the pulse. The phase of Eq. (3), $\psi(f)+\psi(-f)$, is an even function of baseband frequency f, providing all spectral phase components symmetric with respect to carrier frequency f_0:

$$\psi_{e1}(f)\equiv[\psi(f)+\psi(-f)]/2=\angle\widetilde{G}_1'(f)/2. \tag{4}$$

Equation (4) means that a one-dimensional MIFA trace arising from a δ-like PM spectrum is sufficient to retrieve "half" of the spectral phase information. This is attributed to the fact that each frequency component of nonlinear polarization spectrum $P_{NL}(f)$ is associated with the entire pulse spectrum through autoconvolution [12], and spectral sampling of $P_{NL}(f)$ by a narrow $H_1(f)$ still preserves a significant part of the pulse information. This fact that the second harmonic yield at a single frequency depends on the (even-order) spectral phase of a pulsed input has been previously used for waveform discrimination in optical code-division multiple-access communications [15] , but not for waveform measurement. We describe the procedures to obtain the remaining pulse information in the following paragraph.

Complete (second order and higher) spectral phase retrieval can be accomplished if we measure a second MIFA trace $S_2(\tau)$ by using a narrow PM spectrum $H_2(f)$ centered at $2(f_0+\Delta)$ (can be achieved by tuning the PM angle of a birefringent crystal or changing the temperature of a quasi-phase matched grating). The aforementioned procedures give rise to an even function of variable $f+\Delta$ (neither even nor odd in terms of variable f), providing all spectral phase components symmetric with respect to carrier frequency $f_0+\Delta$:

$$\psi_{e2}(f)\equiv[\psi(f)+\psi(-f+2\Delta)]/2, \tag{5}$$

Combining Eq. (4) and Eq. (5), we can derive a recursive relation to reconstruct the spectral phase $\psi(f)$ of the pulse (with a resolution of 2Δ):

$$\psi(f+2\Delta)-\psi(f)=2[\psi_{e2}(f+2\Delta)-\psi_{e1}(f)]. \tag{6}$$

Equations (4) and Eq. (6) show that the capability of spectrally selective "even" phase retrieval of MIFA method allows for analytic phase reconstruction by using two one-dimensional correlation traces. It is worth mentioning that MEFISTO can achieve the same result by taking a two-dimensional interferometric FROG trace, and analyzing the data at two different delay-frequencies [5]. Therefore, these two methods retrieve the spectral phase of the unknown pulse by analyzing the interferometric spectrogram in two different procedures.

Note that the employment of $\cos^{-1}$ function in evaluating $\angle G_1'(\tau)$ results in some limitations. (1) The sign of $\angle G_1'(\tau)$ is ambiguous, causing an ambiguity of the signs of ψ_{e1}, ψ_{e2} (and ψ) for $F\{G_1'(\tau)^*\}=\widetilde{G}_1'(-f)^*=\widetilde{G}_1'(f)^*$. This is analogous to the time-reversal ambiguity of intensity autocorrelation and second-harmonic generation FROG [4]. (2) The value of $\angle G_1'(\tau)$ only lies within $[0,\pi]$, and "sign switching" has to be deliberately imposed whenever the curve $\angle G_1'(\tau)$ meets with 0 or π [16]. An approach to alleviate these problems is using a Michelson interferometer with an unbalanced power splitting ratio $r\neq 1$, where the pulse pair is formulated as: $e_\omega(t)=\sqrt{r}e(t)+e(t-\tau)$. In this case, Eq. (1) can be generalized to:

$$\begin{aligned}S_1(\tau)\propto 1+\frac{4r}{1+r^2}\left|G_1'(\tau)\right|^2+\frac{2r}{1+r^2}\cos(4\pi f_0\tau)+\\ \frac{4\sqrt{r}}{1+r^2}\left\{(r+1)\mathrm{Re}\left[G_1'(\tau)\right]\cdot\cos(2\pi f_0\tau)+(r-1)\mathrm{Im}\left[G_1'(\tau)\right]\cdot\sin(2\pi f_0\tau)\right\},\end{aligned} \tag{7}$$

where Im[ ] denotes imaginary part. By processing the components of $\widetilde{S}_1(\kappa)[=F\{S_1(\tau)\}]$ centered at delay-frequencies of $\kappa=+f_0$ and applying the condition of $G_1'(0)=1$ [see Eq. (2)], we

#103009 - $15.00 USD Received 21 Oct 2008; revised 20 Nov 2008; accepted 22 Nov 2008; published 26 Nov 2008

are able to retrieve Re$[G_1^{'}(\tau)]$, Im$[G_1^{'}(\tau)]$ and the power splitting ratio r as long as the interferometric fringes are properly resolved. This means that an unbalanced Michelson interferometer in MIFA scheme provides additional information [specifically Im$[G_1^{'}(\tau)]$, thus unambiguous $G_1^{'}(\tau)$, $\psi_{ei}(f)$, and $\psi(f)$] [3]. However, a strong power unbalance should be avoided for it will degrade the signal-to-background contrast and overall signal strength in retrieving $G_1^{'}(\tau)$ and $\psi(f)$.

3. Simulation

We assume a chirped pulse with carrier frequency $f_0 = 193.4$ THz ($\lambda_0 = 1550$ nm) and a baseband power spectrum $\widetilde{I} = |A(f)|^2$ of arbitrary shape whose full width at half maximum (FWHM) W is 5 THz (Fig. 2(a), dashed). The spectral phase is assumed as a third-order polynomial $\psi(f) = a(f/W)^2 + b(f/W)^3$ with coefficients of $a = 14, b = 39$, respectively (Fig. 2(a), solid). The performance of spectral phase retrieval is quantitatively measured by the root-mean-square (rms) error defined as: $\varepsilon = \{[\sum(\psi^{'} - \psi)^2 \times \tilde{I}^2]/[\sum \tilde{I}^2]\}^{1/2}$, where ψ and $\psi^{'}$ represent assumed and retrieved spectral phase functions, respectively [17]. To verify the feasibility of MIFA scheme, we assume the two PM spectra $H_1(f)$, $H_2(f)$ as ideal δ-functions centered at $2f_0$ and $2(f_0 + \Delta)$, where $2\Delta = 0.5$ THz. Figures 2(b) and Fig. 2(c) show the two MIFA traces, calculated by Eq. 7 (with power splitting ratio $r = 2$), while Fig. 2(d) and Fig. 2(e) illustrate the corresponding even phase functions $\psi_{e1}(f)$, $\psi_{e2}(f)$ (centered at $f = 0$, $f = \Delta$, respectively). The retrieved spectral phase $\psi^{'}$ (Fig. 2(a), open circles) derived by using Eq. (6) and removing the constant and linear phase terms is in good agreement with the assumed one (solid line), corresponding to a small phase error of $\varepsilon = 8.18 \times 10^{-5}$ rad (limited by finite spectral resolution or sampling window of the simulation). We also assume a π-phase shift for the pulse spectrum (Fig. 2(f), solid) and keep all other parameters intact. This corresponds to a pulse doublet in the time domain [and multiple zero crossings for $G_1^{'}(\tau)$], which is difficult to be reconstructed by iterative Fourier transform algorithm of FROG [18]. In our simulation, the power-unbalanced MIFA scheme can still accurately resolve the phase shift (Fig. 2(f), open circles) with a small phase error of $\varepsilon = 6.13 \times 10^{-5}$ rad.

In the presence of nonzero PM bandwidth, additional error arises from: (1) distortion of two even phase functions ψ_{e1}, ψ_{e2}; and (2) interference of complete phase reconstruction associated with overlapped PM spectra H_1, H_2. To analyze the dependence of measurement error on PM bandwidth, we assume a complex spectrum identical to that of Fig. 2(a), and a series of PM power spectral pairs. Each pair consists of two sinc^2 functions (typically resulting from uniform nonlinear crystals) with a common FWHM of W_{PM} and centered at $2f_0$ and $2(f_0 + \Delta)$ ($2\Delta = 0.1W = 0.5$ THz), respectively (inset of Fig. 3). Under the circumstances, MIFA trace is deviated from Eq. (1) or Eq. (7), and the retrieved spectral phase $\psi_{ei}(i = 1, 2)$ has some error. As shown in Fig. 3, the error values of even phase functions ψ_{ei} (circles and triangles) and complete phase function ψ (squares) steadily increase with PM bandwidth well before the two PM spectra overlap noticeably. It is found that a PM bandwidth in the order of one-tenth of the pulse bandwidth ($W_{PM} \approx 0.1W$) is sufficient to retrieve spectral phase with a small error of $\varepsilon \approx 10^{-1}$ rad. Other simulation (not shown here) indicates that this rough criterion for PM bandwidth also applies for pulses with very different chirp rates. Using an even narrower PM bandwidth (even thicker crystal) improves the measurement accuracy and sensitivity provided that the pulse is not seriously distorted by group velocity dispersion (GVD). The appropriate range of crystal thickness can be determined in the same way as in GRENOUILLE [8]. When the two PM spectra H_1, H_2 are overlapped ($W_{PM} > 2\Delta$), the recursive phase reconstruction process may introduce extra error. According to Eq. (6), this phenomenon limits the resolution of retrieved spectral phase profile $\psi(f)$. The trade-off among the accuracy, sensitivity, and resolution of MIFA scheme should be taken into account in determining the crystal thickness in the experi-

#103009 - $15.00 USD Received 21 Oct 2008; revised 20 Nov 2008; accepted 22 Nov 2008; published 26 Nov 2008

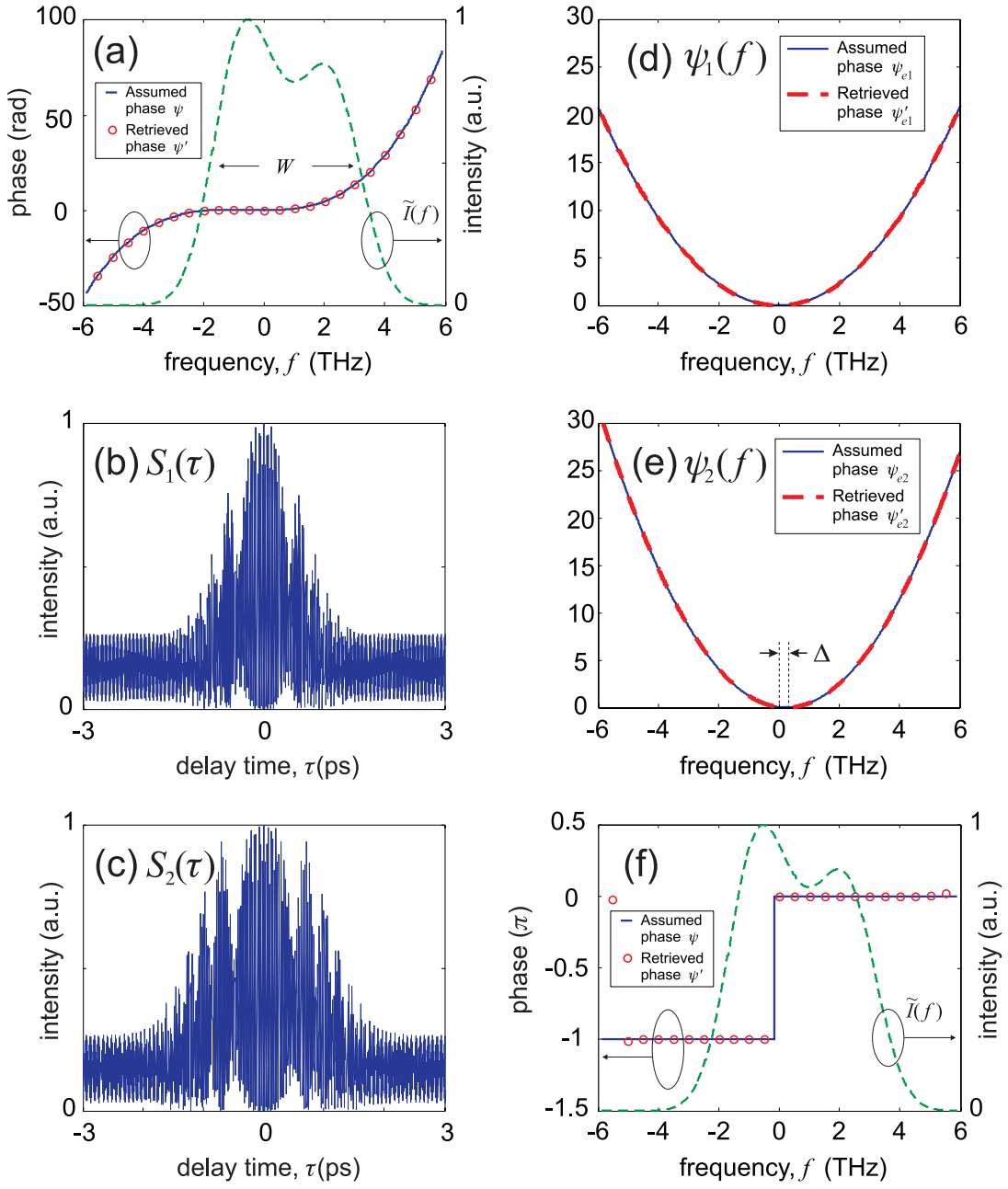

Fig. 2. Theoretical verification of MIFA method. (a) Assumed power spectrum (dash), assumed spectral phase (solid), retrieved spectral phase (open circles). (b-e) The corresponding MIFA traces $S_1(\tau)$, $S_2(\tau)$, and even phases $\psi_{e1}(f)$, $\psi_{e2}(f)$ produced in retrieving spectral phase in (a). (f) Simulation result by assuming π-phase shift. The corresponding rms errors in (a) and (f) are 8.18×10^{-5} rad, and 6.13×10^{-5} rad, respectively.

#103009 - $15.00 USD Received 21 Oct 2008; revised 20 Nov 2008; accepted 22 Nov 2008; published 26 Nov 2008

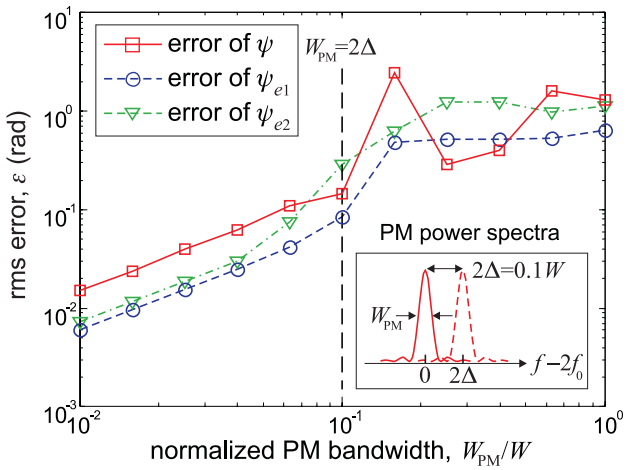

Fig. 3. Rms error of even phase functions ψ_{e1} (circles), ψ_{e2} (triangles), and complete phase ψ (squares) versus normalized PM bandwidth at fixed PM spacing of $2\Delta = 0.5$ THz. Inset shows the definition of PM power spectral pair used in the simulation.

ments.

4. Experiment

The fiber-based experimental setup for MIFA measurement is shown in Fig. 4. The signal pulse comes from a passively mode-locked fiber laser spectrally selected by a filter (Fig. 5(a), solid) or a pulse shaper (Fig. 5(b), solid) at C-band. It is combined with a reference from a CW laser at 1480 nm by a wavelength division multiplexer (W1), then sent into a Michelson interferometer (MI) where an electrically controlled delay line (OZ optics, ODL-650) is used for delay scanning. A second wavelength division multiplexer (W2) and another 3-dB coupler (C3) split the optical wave into three different paths, which are detected by two InGaAs photodetectors (PD1, PD2) and one SHG crystal followed by a Si photodetector (PD3), respectively. The CW reference goes to PD1, producing a trace of sinusoidal fringes $S_{CW}(\tau)$, which can be used to correct irregularly sampled delays of the MI (arising from instability of scanning speed of the delay line). PD2 measures the average power of the signal pulse pair as a function of delay $S_{FA}(\tau)$. By analyzing $S_{FA}(\tau)$ in software, one can obtain the complex field autocorrelation function $\langle a(t)a^*(t-\tau)\rangle$ and signal power spectrum $|A(f)|^2$ without using a spectrometer [19]. In the third path, a fiber-pigtailed periodically poled lithium niobate (PPLN) waveguide [20] (thus free of beam diffraction) with 59-mm-long quasi-phase matched grating is employed as the SHG crystal, providing a PM power spectrum of sinc^2-shape and $\approx$ 50-GHz bandwidth (FWHM), which is sufficient to accurately measure pulses with a bandwidth greater than 0.5 THz. The GVD (defined as $\beta''(f_0)/2$, where β is the propagation constant) of congruent lithium niobate at C-band is $\approx 1.97\times10^{-3}$ ps^2/mm, therefore, our PPLN sample causes an accumulated dispersion of ≈ 0.118 ps^2, which can only broaden the pulses used in our experiments (spectral widths are $\approx$ 1 THz) by $\approx$ 1%. Changing the PPLN temperature around 82.5 °C enables tuning of the central PM wavelength around 1542 nm at a slope of ≈ 0.1 nm/ °C. MIFA trace is obtained by measuring the average second-harmonic power as a function of delay by PD3.

We applied spectral phase modulation on the pulse in two different ways to verify the feasibility of MIFA scheme. (1) A section of 5.15-m-long single mode fiber (Corning SMF-28) was inserted into the link to provide (predominantly) quadratic spectral phase modulation. The even-

#103009 - $15.00 USD Received 21 Oct 2008; revised 20 Nov 2008; accepted 22 Nov 2008; published 26 Nov 2008

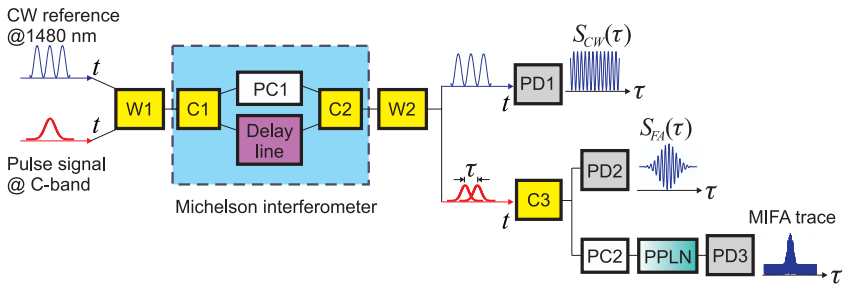

Fig. 4. Experimental setup of MIFA measurement. W#: WDM, C#: 3-dB coupler, PC#: polarization controller, PD1&PD2: InGaAs photodetectors, PD3: Si photodetector.

order spectral phase before(after) the insertion of the SMF, shown as dash(dash-dot) curve in Fig. 5(a) (the quadratic dash curve results from the uncompensated dispersion of the fiber-based apparatus, corresponding to a chirped pulse of $\approx$ 1-ps duration), was obtained by measuring one MIFA trace at fixed PPLN temperature of 107°C (corresponding to 1545-nm central PM wavelength). Here a single temperature was appropriate since the spectral phase was known to be predominantly quadratic. Fitting the spectral phase difference curve over a frequency range of $\approx$ 1 THz gives rise to a quadratic coefficient of c_2 [defined as $\psi(f) = c_2 f^2$] of 2.092 ps^2, close to the prediction of the SMF specification ($D = 17.11$ps/nm/km, or $c_2 = 2.203$ ps^2 at 1545 nm).(2) A Fourier transform pulse shaper was used to impose cubic spectral phase modulation with a coefficient c_3 [defined as $\psi(f) = c_3 f^3$] of 3.721 ps^3 (Fig. 5(b), dash). The complete spectral phase before(after) the employment of pulse shaper was obtained by measuring two MIFA traces at PPLN temperatures of 82.5°C and 80.5°C (corresponding to central PM wavelengths of 1541.9 nm and 1541.6 nm), respectively. The resulting spectral phase difference curve (Fig. 5(b), dash-dot) corresponds to a cubic coefficient c_3 of 3.712 ps^3 (fit over a frequency range of 2 THz), which is in good agreement with the imposed modulation function. Note that the power spectrum (Fig. 5(b), solid) obtained via analysis of the electric field autocorrelation contains several dips arising from diffraction effects induced by abrupt phase changes in the pulse shaper. The good agreement of the retrieved spectral phase with the phase applied by the shaper shows that the MIFA technique is applicable even to pulses with nontrivial power spectra.

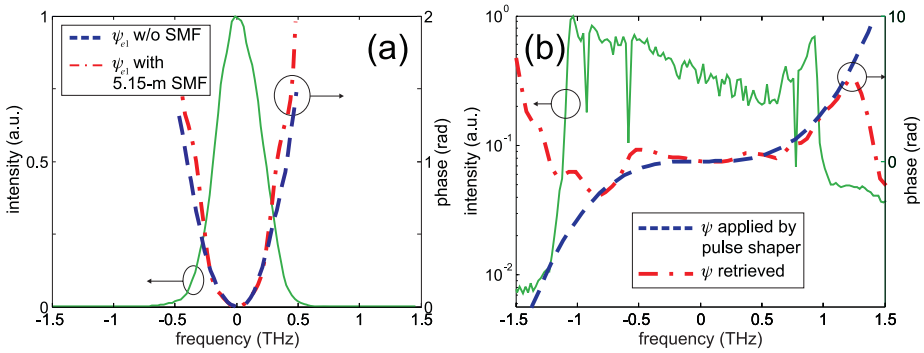

Fig. 5. (a) Even-order spectral phase before (dash) and after (dash-dot) the insertion of 5.15-m-long SMF. (b) Complete spectral phase imposed by pulse shaper (dash) and retrieved by MIFA scheme (dash-dot).

#103009 - $15.00 USD Received 21 Oct 2008; revised 20 Nov 2008; accepted 22 Nov 2008; published 26 Nov 2008

5. Conclusion

In conclusion, we have demonstrated that one-dimensional interferometric autocorrelation traces measured by using thick nonlinear crystals are sufficient to directly reconstruct the spectral phase of ultrashort pulses. An important point is that this measurement technique is non-iterative and compatible with (in fact enabled by) a second harmonic generation interaction with narrow phase matching bandwidth. In addition to its novelty, this self-referenced method has inherent potential for high measurement sensitivity because of the long nonlinear interaction length. Such potential can be realized without the need for the custom aperiodically poled waveguide devices used in the high sensitivity measurement experiments of [9,10,11,12]. Aside from the nonlinear crystal, our measurement setup only requires a standard collinear Michelson interferometer and point detectors, thus sparing the expense of a spectrometer and detector array. The efficiency and precision of interferometric fringe analysis procedures can be further improved by using the powerful wavelet algorithm [21].

Acknowledgments

We thank Dr. R. V. Roussev, Dr. C. Langrock, Dr. M. M. Fejer for providing us the PPLN waveguide, and Dr. D. E. Leaird, Dr. Y. -W. Hong for their technical support and constructive comments. This material is based upon work supported by National Science Council of Taiwan under grant 96-2112-M-007-016. The work of H. Miao, C. -B Huang, and A. M. Weiner at Purdue University was supported in part by the National Science Foundation under grants 0501366-ECS and 0601692-ECCS.

#103009 - $15.00 USD Received 21 Oct 2008; revised 20 Nov 2008; accepted 22 Nov 2008; published 26 Nov 2008